Impacts of Polystyrene Molecular Weight and Modification to the Repeat Unit Structure on the Glass Transition−Nanoconfinement Effect and the Cooperativity Length Scale

Christopher J. Ellison,[†] **Manish K. Mundra,**[‡] **and John M. Torkelson***[,†,‡]

Department of Chemical and Biological Engineering and Department of Materials Science and Engineering, Northwestern University, Evanston, Illinois 60208-3120

Received October 18, 2004; Revised Manuscript Received December 12, 2004

ABSTRACT: The effect of nanoconfinement on the glass transition temperature (T_g) of supported polystyrene (PS) films is investigated over a broad molecular weight (MW) range of 5000−3 000 000 g/mol. Polystyrene MW is shown to have no significant impact on the film thickness dependence of $T_g - T_{g,bulk}$. In contrast, a small modification to the repeat unit structure of PS has a dramatic impact on the T_g-nanoconfinement effect. The strength of the thickness dependence of T_g is greater for poly(4-methylstyrene) (P4MS) than for PS and yet much greater for poly(4-*tert*-butylstyrene) (PTBS). The T_g reduction for PTBS is 47 K below $T_{g,bulk}$ for a 25 nm thick film, with the onset thickness for confinement effects in PTBS being 300−400 nm. Measurements of the size of cooperatively rearranging regions, $\xi_{CRR,}$ in bulk polymer systems at T_g reveal that PS MW has no significant effect on ξ_{CRR} unless PS is oligomeric or nearly oligomeric. However, changes to repeat unit structure and diluent addition affect ξ_{CRR} values, but not in a manner that yields an obvious correlation with the T_g-nanoconfinement effect.

Introduction

When confined to nanoscale dimension, both low molecular weight[1−6] and polymeric[7−36] glass formers have been widely observed to exhibit glass transition temperatures (T_gs) that deviate substantially from their bulk values. This behavior has implications in applications such as photoresists, disk drive lubricants, asymmetric membranes, and nanocomposites, among others. This broadly based technological impact and the strong dependence of many key material properties (mechanical, viscoelastic, diffusive, etc.) on the proximity of temperature to T_g have driven research efforts in this area. Thin and ultrathin films have dominated research into nanoconfined polymer behavior due to the ease with which the confining dimension, film thickness, can be varied. Polymer films may be supported by a substrate[7−24,30−37] or freely standing (unsupported).[13,14,26−29] For freely standing films, T_g decreases with decreasing film thickness. In contrast, for supported polymer films, increases in T_g for polymers with strong attractive substrate interactions[8,9,14−16,22,23,35] and decreases in T_g for polymers with neutral or repulsive substrate interactions[7,8,10−24,32,34−36] have been observed with decreasing thickness. In a few cases involving copolymers with comonomer units that exhibit attractive and neutral or repulsive substrate interactions, T_g has been observed to be nearly invariant with film thickness.[33,37] Various methods have been used to characterize T_g in polymer films, including dielectric relaxation spectroscopy,[12,30,31] fluorescence spectroscopy,[22−25] Brillouin scattering,[13,26−28] ellipsometry,[7,8,10,13,15−20,29,32−35] X-ray reflectivity,[9,21,35,36] and nonlinear optics.[37]

Many postulates have been offered regarding the origin of these effects[14] in systems lacking attractive polymer−substrate interactions: internal stresses caused by film preparation methods (e.g., spin-coating);[38,39] a "finite size effect" due to the thickness approaching a fundamental length scale associated with glass formers,[7] e.g., the cooperatively rearranging region (CRR) introduced by Adam and Gibbs;[40] interfacial effects involving a reduced entanglement concentration[18,38,39,41] or a segregation of chain ends to the free surface (air−polymer interface);[18,42] and a radius of gyration (R_g) that is on the order or a small multiple of the film thickness, h.[20,29] With supported polystyrene (PS) films, two reviews[10,14] have found extensive agreement for the T_g-nanoconfinement effect across many measurement methods: when scaled according to the bulk T_g as $T_g(h)/T_{g,bulk}$,[43] the thickness dependence of T_g has been found to be approximately independent of PS molecular weight (MW)[10−12,14,18] over a MW range of 3600−2 900 000 g/mol.

The notion that internal stresses cause the T_g-nanoconfinement effect may be refuted by the agreement among many studies of supported PS films[10,14] in which films of similar thickness were prepared using different solutions (solvent type and polymer concentration) and preparation conditions (spin-coating speed). However, related studies of ultrathin PS[44,45] and polycarbonate[46] films have shown the existence of a negative thermal expansivity in the glassy state which has been attributed to a nonrelaxed structure that is set in during spin-coating.[21,44] This effect, which exhibits little impact on T_g,[44] can be removed by annealing at $T_{g,bulk}$ + 50 K for 2 h.[21,44]

There has been interest[14] in connecting the size scale at which nanoconfinement effects are observed to the size scale of a CRR. (Adam and Gibbs[40] introduced the concept of a CRR in which local relaxation occurs by the collective motion of many molecules or polymer segments.) The length scale of a CRR near T_g has been investigated by differential scanning calorimetry,[47−52] 4D NMR,[53,54] and other techniques[55,56] and has been reported to lie in the range of ~1−4 nm for low MW and polymeric glass formers. However, the length scale

† Department of Chemical and Biological Engineering.
‡ Department of Materials Science and Engineering.
* To whom correspondence should be addressed: e-mail j-torkelson@northwestern.edu.

10.1021/ma047846y CCC: $30.25
Published on Web 02/03/2005

at which nanoconfinement effects are observed is ~10 nm or less for low MW glass formers[1-6] and ranges from several tens to more than one hundred nanometers for polymers.[7-37] This indicates that the length scale of a single CRR is far less than the thickness at which T_g-nanoconfinement effects are observed.

Recent understanding gained from fluorescence experiments[24] has reiterated this point. These experiments have revealed via multilayer PS films with fluorescent labels in only one layer that the free surface effect causes a T_g reduction that persists several tens of nanometers into the film interior (much larger than a single CRR). Furthermore, it was observed[24] that a region of reduced T_g near the free surface exists as a continuous distribution of T_gs that depends on the degree of nanoconfinement. These results have shown directly that two-layer and three-layer models[9-12,14,27] are inadequate to explain T_g-nanoconfinement behavior and that a model that incorporates a continuous distribution of T_gs across the thickness of a film is needed. This picture is consistent with recent simulations[57] and predictions from theoretical pictures.[58,59]

Many other studies[6,8,14,17,60-64] have indicated that interfacial effects are the most logical explanation for the underlying cause of the T_g-nanoconfinement effect. Numerous studies have concluded[24,57-64] that the free-surface T_g of bulk PS films is some tens of degrees lower than the bulk T_g. Supporting the importance of free-surface effects for PS, a recent study[17] has shown that removing the free-surface interface by placement of Al or Au metal onto the film results in a T_g that is independent of thickness down to 10 nm or less. The key role of interfacial effects is also supported by studies of the thickness dependence of T_g for polymers with attractive substrate interactions,[8,9,15,16,22,23,33] e.g., poly(2-vinylpyridine) and poly(methyl methacrylate) on silicon (with native oxide) or glass substrates which exhibit increases in T_g with decreasing thickness due to the attractive substrate interactions.

Although there is substantial evidence supporting a free-surface effect as the origin of T_g reductions in nanoconfined PS films, there is not yet a detailed understanding of the free-surface effect. A simple explanation is that polymer segments that lie at the free surface possess fewer conformational restrictions than those in the bulk and thus have a higher degree of cooperative segmental mobility and an associated lower T_g. While this explanation is logical, it lacks details regarding the extent to which interfaces may be expected to modify cooperative segmental mobility or T_g from that of bulk. Others have offered the explanation that the free surface results in a reduced entanglement concentration,[18,38,39,41] which in turn yields enhanced mobility and reduced T_g near the free surface. However, this explanation can be criticized because a thickness-dependent T_g has been observed for both entangled and unentangled PS[10-12,14,18] (M_c, the critical entanglement MW, is ~35 000−38 000 g/mol[65,66] for PS) and because bulk T_g does not depend on chain entanglements.[65]

Another potential explanation involves the segregation of chain ends to the free surface that would be expected to reduce the local T_g at the free surface.[18,42] However, if chain ends were the origin of this effect, it would be expected that the thickness dependence of T_g could be significantly altered by varying the surface chain-end concentration by modification of the polymer MW,[42] which is not supported by experimental data. Variation of polymer MW also greatly alters the R_g of the bulk polymer, which in turn would significantly affect the film thickness at which overall chain conformation would be expected to differ substantially from bulk. For example, when PS MW is increased from 3600 to 2 900 000 g/mol, the bulk R_g increases from ~2 to 47 nm (using a characteristic ratio of 10 to calculate R_g[65,67]).[68] Some have argued that such an effect may yield a MW dependence of the T_g-nanoconfinement effect.[20,30] In opposition to this picture is a large body of evidence[10-12,14,18] indicating that the T_g-nanoconfinement effect for supported PS films is approximately independent of MW; this means that neither chain ends nor bulk R_g plays a significant role in defining this effect.

It is noteworthy that two very recent studies[20,21] of supported PS films have reported a MW dependence of the T_g-nanoconfinement effect in the range of 212 000−2 900 000 g/mol.[69] Singh et al.[20] reported that the thickness dependence of T_g for a variety of PS MWs can be collapsed onto a master curve when thickness is scaled as h/R_g(bulk) and T_g is scaled as $T_g(h)/T_{g,bulk}$. While the study by Miyazaki et al.[21] was largely focused on thermal expansion effects, it also reported a larger T_g-nanoconfinement in ultrathin films of higher MW (2 890 000 vs 303 000 g/mol) PS down to ~10 nm in thickness.

As a result of this recent disagreement regarding the impact of MW on the T_g-nanoconfinement effect in supported PS films as well as the results of our study[25] showing that this effect can be dramatically reduced by addition of low MW diluents, we have chosen to study the tunability of the T_g-nanoconfinement effect by making small changes to the molecular structure of PS. We have also investigated the effects of these changes in molecular structure on the cooperativity length scale at T_g. The changes in structure include the largest range of MWs examined to date in a single study of supported PS films as well as modifications to the repeat unit involving a comparison of PS to P4MS and PTBS, all supported on glass substrates.

Experimental Section

Polystyrene standards were purchased from Polysciences Inc. and Pressure Chemical Co. and used as received. Samples of PS films with M_n = 5000 g/mol were prepared by codissolving a high MW PS standard (M_n = 200 000 g/mol) with a low MW PS standard (M_n = 1850 g/mol) in toluene (99.9% purity) prior to film preparation. Pyrene-labeled PS was synthesized by copolymerizing a 1-pyrenylbutyl methacrylate with styrene, resulting in a polymer with 1 in 170 repeat units being a pyrene-labeled methacrylate; details of the synthesis are reported elsewhere.[24] Poly(4-methylstyrene) (P4MS) was from Scientific Polymer Products and used as received. Poly(4-*tert*-butylstyrene) (PTBS), poly(vinyl acetate) (PVAc), and glycerol (99.5+%) were from Aldrich. Because of the presence of 4-*tert*-butylstyrene monomer in the as-received polymer, the PTBS sample was dissolved in toluene (99.9% purity) and precipitated seven times in methanol (99.9% purity) to ensure monomer removal prior to use. $T_{g,bulk}$ values were measured as $T_{g,onset}$ values by differential scanning calorimetry (DSC) (Mettler Toledo DSC822) on second heat at 10 K/min. Polymer MW was determined by gel permeation chromatography (GPC) (Waters) relative to a PS calibration unless otherwise noted. Table 1 provides details on values of sample M_n, M_w/M_n, and $T_{g,bulk}$ by DSC and $T_{g,bulk}$ as determined by this fluorescence method. Pyrene (Aldrich Chemical, 99+% purity), 1,10-bis(1-pyrene)decane (BPD) (Molecular Probes), and dioctyl phthalate (DOP) (Aldrich, 99%) were used as received.

Table 1. Molecular Weight and Bulk T_g for Materials Employed in This Study

material	M_n (g/mol)	M_w/M_n	$T_{g,bulk}$ (K) (onset, DSC)	$T_{g,bulk}$ (K) (fluor)
PS	23000000	1.30	374	
PS	3000000	1.05	374	373
PS	400000	1.06	375	
PS	263000	1.10	373	373
PS	200000	1.08	373	373
PS	13500	1.06	368	
PS	12000	1.10	365	364
PS	5000	bimodal[a]	358	358
PS	1850	1.14	333	
PS	800	1.11	269	
PS	568	1.13	248	
P4MS	279000	1.57	376	376
PTBS	32000	3.31	404	404
PS w/pyrene label	440000	1.73	369	371
glycerol			188	

[a] Blend of 1850 and 200000 g/mol PS.

Thin films were prepared by spin-coating[70] dilute solutions of polymer in toluene (Fisher, used as received) onto glass slides. The slides were initially washed with a 10% sodium hydroxide/70% ethanol/20% water solution[22] and then solvent washed between experiments. Film thickness was measured with a Tencor P10 profilometer. Calibration of the profilometer was verified using a 14 nm step-height standard (VLSI standards). At least 10 measurements were taken in total at different locations close to the center of the film (where fluorescence was measured) and averaged with the typical standard deviation in these measurements being less than 1.5 nm for films thicker than ~20 nm and ~1.0 nm for films thinner than ~20 nm.

A Spex Fluorolog-2DM1B fluorimeter was used for steady-state fluorescence measurements. Measurements employed front-faced geometry with 2.5 mm excitation and emission slits (band-pass = 4.5 nm) for films with thickness < 100 nm and 1.25 mm excitation and emission slits (band-pass = 2.25 nm) for films with thickness > 100 nm. In the worst case, the signal-to-noise ratio exceeded 30. The probe (pyrene or BPD) content in each film was <0.2 wt % of dry polymer content. (At this probe concentration the T_g value of pyrene-doped polymer is the same within error as that of neat polymer, a circumstance that also holds for BPD.) A clean quartz cover slide was placed on top of each film to reduce the potential for probe sublimation during the T_g measurement by fluorescence. (The film was adhered only to the glass substrate on which it was spin-coated.) Film temperature was controlled by a microprocessor controller (Minco Products) with a Kapton ribbon heater attached to a flat aluminum plate that was also used as a clamping device to hold the sample. The excitation wavelength was 322 nm for all samples, and the emission spectrum was measured at 350−450 nm. No excimer fluorescence was observed in any sample. Fluorescence spectra were recorded upon cooling after having annealed samples at $\sim T_g + 40$ K for 15 min. In the case of the PS with M_n = 3 000 000 g/mol, samples were annealed at $\sim T_g + 40$ K for 45 min; in the case of PS with $M_n \leq$ 12 000 g/mol, dewetting problems were reduced or eliminated by annealing for 15 min at $\sim T_g + 35$ K.

In fitting the temperature dependence of fluorescence in the rubbery and glassy states, only data points well outside T_g were used for the linear fits, and typical correlation coefficients (R^2) were better than 0.990. To initiate the fitting procedure, data points were added to the rubbery- and glassy-state linear regressions at the extrema in the temperature range of the data. The correlation coefficient was monitored as more data points were added (approaching T_g from the extrema in the temperature range of the data) to each of the linear regressions. If the R^2 value began to steadily decrease below a threshold value (i.e., <0.990) as more data points were added, then these data points were removed to produce a value of R^2 higher than the threshold value, and the linear regressions were considered acceptable. The linear fits in both the rubbery and glassy states included a minimum of four fluorescence data points (usually more), spanning a minimum of 15 K in temperature. This procedure was followed regardless of whether fitting linear functions to the fluorescence intensity data at particular emission wavelength(s) or the integrated intensity as a function of temperature. When using integrated intensities to identify T_g (the usual case), spectra were taken over a sufficient range of wavelengths that integration could be done from instrument baseline at the lowest wavelengths to the same instrument baseline at the highest wavelengths.

When fitting the temperature dependence of the fluorescence intensity data at the peaks in the emission spectra (as done previously in refs 22−25), the standard deviation in the determination of T_g at the various peaks in the emission spectra was typically less than 1.0 K for each sample. This is comparable to the estimated standard variation (or error) in T_g (±1.0 K or less) from sample to sample (identified either using intensities or integrated intensities) for films of identical thickness on identical substrates when the film thickness is greater than ~25 nm. As film thickness decreased below ~25 nm, the estimated standard variation (or error) is estimated to be ±2 K. Further details on measurement of T_g by fluorescence are given elsewhere.[22−25]

Differential scanning calorimetry (Mettler Toledo DSC822) was used to measure the heat capacity for the determination of the size of the CRR.[47,48] Initially, the furnace was heated to 973 K in the presence of oxygen to oxidize any impurity present from previous use. Specific heat capacities were measured against a sapphire standard. A blank pan was run followed by a sapphire standard immediately prior to characterization of each polymer sample. The calibration of the DSC instrument was regularly monitored via an indium standard. All DSC measurements were taken on the second heating (10 K/min) cycle after quenching (40 K/min) from elevated temperature. Samples were annealed for at least 45 min at the elevated temperature (353 K for PS M_n = 800 g/mol and PS M_n = 568 g/mol and 473 K for the other samples) before quenching to erase prior thermal history and, even more importantly, to optimize sample-pan contact. All thermograms used in heat capacity measurements and thereby the determination of the size of the CRR were taken from $T_{g,bulk} - 70$ K to $T_{g,bulk} + 70$ K in order to measure baselines accurately. The reported heat capacity values are averages of a minimum of six runs. Further details are available in the Supporting Information for this paper.

Results and Discussion

Comparison of T_g-Nanoconfinement Effects as a Function of PS MW. Figure 1a shows the fluorescence emission spectrum of pyrene dopant in an 810 nm thick PS film. There is a significant reduction in overall intensity with increasing temperature (T). Previous studies have shown[22−25] that T_g values can be obtained by plotting the intensity near one or several of the peak wavelengths (~374, 385, and 395 nm) as a function of T. Over a 70−80 K T range roughly centered at T_g, two linear T dependences of intensity are observed, a stronger one in the rubbery state and a weaker one in the glassy state, with the intersection being identified as T_g. Careful inspection of Figure 1a reveals that the exact values of the two slopes in such a plot may depend on the emission wavelength selected because the T dependence of intensity is stronger at the maxima (peaks) than at the minima (valleys) of the emission spectrum. Such effects have been observed by others[71,72] studying the T dependence of pyrene fluorescence in various polymers and can be attributed to the T dependence of the different vibronic bands of pyrene. In addition to these effects, there are slight blue shifts in the emission spectrum of pyrene (1−2 nm) as T is

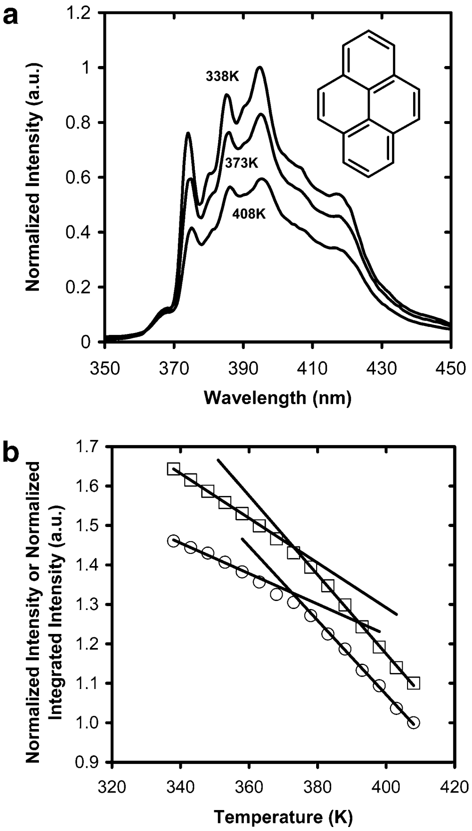

Figure 1. (a) Fluorescence emission spectra of pyrene dopant (<0.2 wt %) in an 810 nm thick PS (M_n = 200 000 g/mol) film taken at 338, 373, and 408 K. The inset shows the structure of pyrene. (b) T dependence of the fluorescence intensity (○) monitored at an emission wavelength of 400 nm and integrated intensity (□) of pyrene dopant in an 810 nm thick PS film (M_n = 200 000 g/mol, $T_{g,bulk}$ = 373 K). (The intensity and integrated intensity have been normalized to one at 408 K and arbitrarily shifted.)

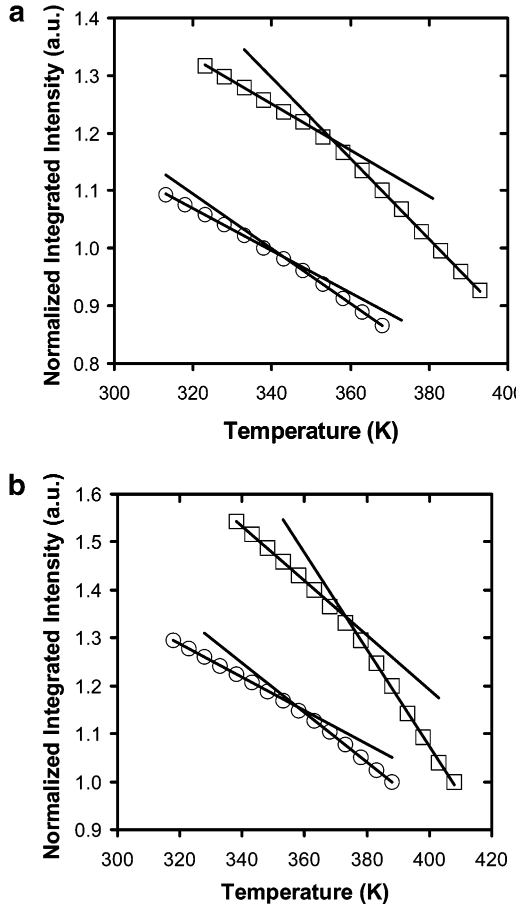

Figure 2. (a) T dependence of the integrated intensity of pyrene dopant in 500 nm thick (□) and 29 nm thick (○) PS (M_n = 5000 g/mol, $T_{g,bulk}$ = 358 K) films. (The integrated intensity has been normalized to one at 368 and 338 K, respectively, and arbitrarily shifted.) (b) T dependence of the integrated intensity of pyrene dopant in 810 nm thick (□) and 24 nm thick (○) PS (M_n = 200 000 g/mol, $T_{g,bulk}$ = 373 K) films. (The integrated intensity has been normalized to one at 408 and 388 K, respectively, and arbitrarily shifted.)

decreased from 413 to 333 K. To minimize these effects, we have chosen to plot values of integrated intensity as a function of T. Figure 1b compares the T dependence of integrated intensity to that of intensity at 400 nm; while the same T_g value (373 K) is determined from both plots, there is a discernible difference in the T dependences of intensity at 400 nm and the integrated intensity over a common T range.

Figure 2a shows the T dependence of integrated intensity for PS with M_n = 5000 g/mol at two thicknesses (500 and 29 nm, T_g = 356 and 344 K, respectively). Similarly, Figure 2b shows a higher MW PS with M_n = 200 000 g/mol at two thicknesses (24 and 810 nm, T_g = 358 and 373 K, respectively). In accord with earlier fluorescence studies[22−25] of the T_g-nanoconfinement effect as well as other studies,[10] these figures demonstrate a weakening in the strength of T_g in highly nanoconfined PS films. In the studies conducted here, a weakening in the strength of T_g for PS is observed with decreasing thickness for films less than ∼30 nm thick, independent of PS MW. Associated with this strength of T_g effect, the error in estimating T_g values by the intersection of linear temperature dependences of integrated intensity in the rubbery and glassy states is ∼±1 K when film thickness is greater than ∼20−25 nm and ∼±2 K when film thickness is less than ∼20−25 nm.

Figure 3 shows the thickness dependence of T_g for PS M_n values ranging from 5000 to 3 000 000 g/mol, which is the broadest range in MWs ever examined in a single T_g-nanoconfinement study. The data in Figure 3 indicate that there is no significant MW dependence over a broad range in PS MWs within the error of these measurements. The solid curve in Figure 3 represents a fit of all the PS data to the relation $T_g(h) = T_{g,bulk}(1 - (A/h)^{\delta})$ originally proposed by Keddie et al.[7] with A = 3.2 nm and δ = 1.63. (The apparent differences in the data for the thinnest films of the 5000 and 3 000 000 g/mol samples should not be taken as significant. There is a ±1 nm uncertainty associated with those film thicknesses, and in the thinnest films this level of uncertainty has a very substantial effect in the extent of the T_g reduction relative to $T_{g,bulk}$. That factor, combined with the ±2 K uncertainty in assigning the T_g value in films less than 20 nm in thickness, is sufficient to indicate that any apparent difference of the T_g-nanoconfinement effect as a function of PS MW is not significant, given the inherent quality of the data.)

This demonstration of the independence of the T_g-nanoconfinement effect with respect to MW in supported PS films is consistent with many previous reports[10−12,14,18] covering a M_n range of 3600−2 900 000 g/mol but is in contradiction with two very recent studies[20,21] that have reported some MW dependence in the range of 212 000−2 900 000 g/mol. It is noteworthy that these two very

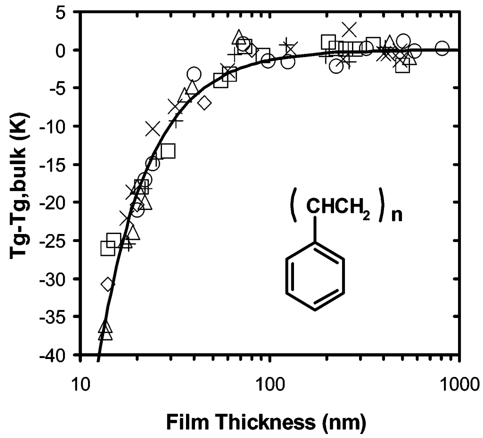

Figure 3. $T_g - T_{g,bulk}$ as a function of film thickness for PS [M_n = 5000 g/mol (□), M_n = 12 000 g/mol (+), M_n = 200 000 g/mol (○), M_n = 263 000 g/mol (×) (reported previously in refs 22−25), M_n = 3 000 000 g/mol (◇)] films as measured by pyrene dopant fluorescence and PS [M_n = 440 000 g/mol (△)] as measured by pyrene label fluorescence (reported previously in ref 24). The curve represents a least-squares fit of the data to the empirical relation originally proposed by Keddie et al.,[7] yielding parameter values $A = 3.2$ nm and $\delta = 1.63$. The inset shows the structure of the PS repeat unit.

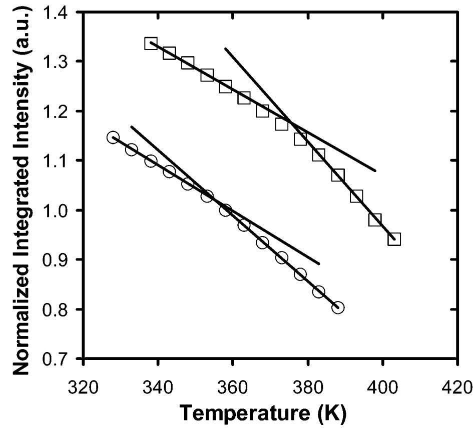

Figure 4. T dependence of the integrated intensity of pyrene dopant in 810 nm thick (□) and 24 nm thick (○) P4MS films ($T_{g,bulk}$ = 376 K) films. (The integrated intensity has been normalized to one at 368 and 358 K, respectively, and arbitrarily shifted.)

recent studies are in some disagreement regarding how PS MW impacts the T_g-nanoconfinement effect. For example, Singh et al.[20] reported a T_g for 100 nm thick films that is 3 K lower for 1 600 000 g/mol PS than for 560 000 g/mol PS with a maximum difference of ∼4 K between T_g values among PS MWs at any particular thickness. In contrast, Miyazaki et al.[21] reported no T_g difference (within error) between 303 000 and 2 890 000 g/mol PS in 100 nm thick films but about a 7 K maximum difference for 20 nm thick films. (Some of the T_g data from Miyazaki et al.[21] have large error bars, bringing into question the extent to which there is a true statistical difference in nanoconfined T_g values as a function of MW.)

At present, the cause for the disagreement between the many studies, including the present one, indicating that there is no significant MW dependence of the T_g-nanoconfinement effect in supported PS films and the two other recent studies indicating the opposite is not known. However, it is noteworthy that Fukao and coworkers[12,30] had concluded in 1999 and 2000 that there was some MW dependence to the T_g-nanoconfinement effect in supported PS films but later concluded[31] in 2002 that there was no MW dependence, which may be an indication of the difficulty in obtaining the highest quality data from what may be deceptively simple studies. A factor that may contribute to the different results obtained by Singh et al.[20] and by Miyazaki et al.[21] is that their studies reported T_g data taken upon heating from the glassy state after a 10 K/10 min step-and-hold method[20,21] while most other studies, including the present one, have been taken upon cooling from the rubbery state. Measuring T_g upon cooling eliminates issues regarding how physical aging, which itself may be a function of thickness in nanoconfined films,[22,73,74] affects the measured T_g. In any case, we believe that the excellent agreement reported in Figure 3 among the many samples with M_n values over a broader range than in any previous single study provides ample evidence of the lack of a significant MW dependence to the T_g-nanoconfinement effect in supported PS films. As such, these results provide further evidence that neither a reduction in entanglement concentration with a reduction in film thickness nor a modification of R_g upon confinement plays a significant role in the thickness dependence of T_g. Furthermore, the fact that the results obtained with the PS sample with M_n = 5000 g/mol, made from a blend of high and very low MW PS standards, agree with those of many nearly monodisperse PS standards effectively demonstrates that chain end segregation plays no significant role in the T_g-nanoconfinement effect. (It should be noted that the concentration of chain ends in a bulk system is only dependent on M_n. However, in a film made of a blend of very low MW and high MW polymer, it is possible[42] that the very low MW PS will segregate to the free surface or air−polymer interface, thereby dramatically increasing the chain end concentration near the surface beyond that expected in a monodisperse system with identical M_n.)

B. Comparison of T_g-Nanoconfinement Effects as a Function of Repeat Unit Structure. In contrast to the independence of the T_g-nanoconfinement effect to PS MW reported in section A, in this section we demonstrate that modifications to the repeat unit structure can significantly impact the T_g-nanoconfinement effect in styrene-based polymers. In particular, P4MS and PTBS systems are compared with PS.

Figure 4 shows the T dependence of the integrated intensity for pyrene-doped P4MS at two thicknesses. Similar to the PS case, P4MS shows a reduced strength in T_g in highly nanoconfined films. (As with PS, a weakening in the strength of T_g for P4MS is observed with decreasing thickness for films less than ∼30 nm thick.) The 24 nm thick and 810 nm thick P4MS films display T_gs of ∼ 355 and 376 K, respectively. In the case of films of thickness less than 25 nm, the estimated error in T_g is ∼±2 K while for thicker films it is ∼±1 K.

Figure 5 shows the thickness dependence of T_g for P4MS compared to the PS data fit to the empirical function from Keddie et al.[7] as shown in Figure 3. For 24 nm thick films, P4MS exhibits a T_g value that is reduced by 21 K relative to $T_{g,bulk}$ while PS exhibits a T_g value that is reduced by ∼14 K relative to $T_{g,bulk}$. This indicates that the addition of one methyl unit on the 4-position of the phenyl ring in the PS repeat unit can have a significant effect on the thickness dependence of T_g. However, it is interesting to note that the onset

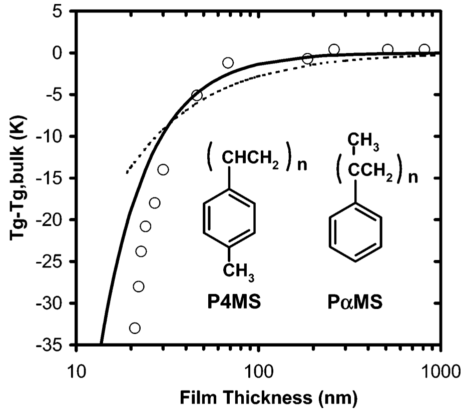

Figure 5. $T_g - T_{g,bulk}$ as a function of film thickness for P4MS (○) films as measured by pyrene dopant fluorescence. The bold curve represents a least-squares fit of the PS data (refer to Figure 3) to the empirical relation of Keddie et al.[7] with parameter values $A = 3.2$ nm and $\delta = 1.63$; the dotted curve is a reproduction of the curve reported in a study of PαMS T_g-nanoconfinement effects (ref 19). The inset shows the P4MS and PαMS repeat unit structures.

thickness at which T_g begins to show a significant deviation from $T_{g,bulk}$, which we define to be a 3 K reduction relative to $T_{g,bulk}$, is virtually the same (~45−50 nm) for P4MS and PS.

Kim et al.[19] have reported on the T_g-nanoconfinement effect observed in poly(α-methylstyrene) (PαMS), in which a methyl unit is located on the α-carbon along the chain backbone. Their data indicate that the onset thickness of the T_g reduction is greater (~90−95 nm) for PαMS than for PS or P4MS. In addition, the shape of the thickness dependence of T_g for PαMS differs from that of PS or P4MS, decreasing much less steeply at thicknesses less than 40 nm. In agreement with our PS results, Kim et al.[19] reported no effect of MW on the reduction of T_g as a function of thickness for PαMS with MWs of 23 000 and 450 000 g/mol.

We have also used fluorescence to measure the T_g-nanoconfinement effect in PTBS, which differs from the repeat unit structure of PS by the addition of a *tert*-butyl group to the 4-carbon on the phenyl ring. The addition of the *tert*-butyl group reduces the bulk density of the polymer by 10% compared to PS (from 1.04 to 0.94 g/cm^3) and increases bulk T_g from ~373 to 404 K. In contrast, the densities and T_g values of P4MS and PS are nearly identical. This decreased density in PTBS may be attributed to significantly hindered packing of the repeat units of PTBS relative to PS which results in an increased free volume. Likely associated with these differences, we have observed that pyrene dopant is particularly susceptible to sublimation from PTBS films during annealing of the film above T_g. To avoid sublimation issues, BPD, shown as the inset in Figure 6a, was chosen as a fluorescence dopant as it has diffusion coefficient in polymers near T_g that is several orders of magnitude lower than that of pyrene.[75] Various tests in PTBS indicated that BPD exhibits relatively little sublimation in the T range of interest.

Figure 6a shows the T dependence of the fluorescence emission spectra for BPD doped at trace levels (<0.2 wt %) into a 1190 nm thick PTBS film. The BPD dopant spectral shape is roughly similar to that of pyrene dopant in PS, with emission peaks at ~378, 398, and 418 nm. Figure 6b shows the T dependence of the integrated intensities for two BPD-doped PTBS films; the 1190 nm thick film exhibits a T_g value of 404 K,

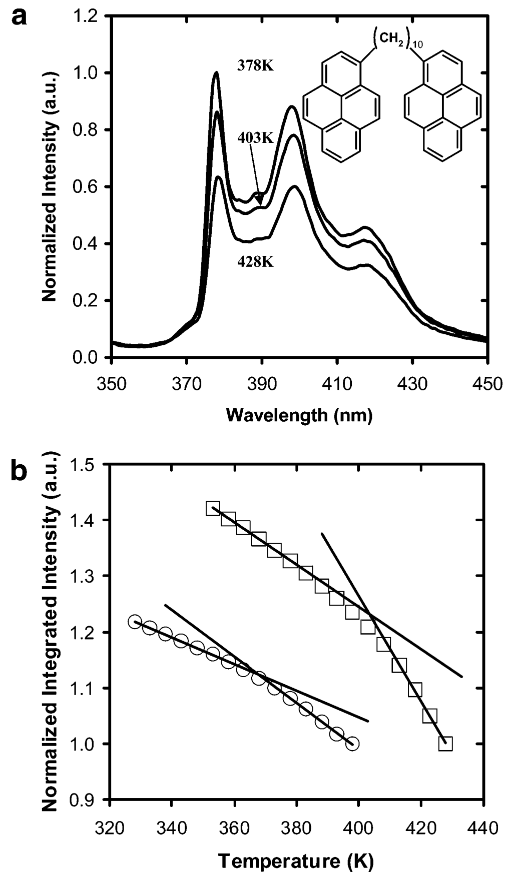

Figure 6. (a) Fluorescence emission spectra of BPD dopant in a 1190 nm thick PTBS film taken at 378, 403, and 428 K. The inset shows the structure of BPD. (b) T dependence of the integrated intensity of BPD dopant in 1190 nm thick (□) and 30 nm thick (○) PTBS ($T_{g,bulk}$ = 404 K) films. (The integrated intensity has been normalized to one at 428 and 398 K, respectively, and arbitrarily shifted).

equal to $T_{g,bulk}$, while the 30 nm thick film exhibits a T_g of 368 K. The 30 nm thick PTBS film also shows a reduction in the strength of T_g compared to the 1190 nm thick film, qualitatively consistent with that shown for PS in Figures 2a,b and P4MS shown in Figure 4. (A weakening in the strength of T_g for PTBS is observed with decreasing thickness for films less than ~30−35 nm thick. The estimated error in the determination of T_g is ±1 K for films with thickness exceeding 30 nm and ±2 K for thinner films.)

Figure 7 compares the thickness dependence of T_g for PTBS and the dependences for P4MS and PS. Also shown are the T_g values of two 200 000 g/mol PS films doped with BPD, showing that BPD and pyrene dopant measure a consistent thickness dependence of T_g in PS. Figure 7 makes clear that there are dramatic differences in the T_g-nanoconfinement effect of PTBS as compared to that of either PS or P4MS. First, the onset thickness for T_g reduction in PTBS, estimated from Figure 7 to be 300−400 nm, is much larger than in PS or P4MS. (Strikingly, this value of onset thickness indicates that the effect is not necessarily limited to the "nano" length scale, often taken as 100 nm or less.) To the best of our knowledge, this is the largest thickness at which the T_g-nanoconfinement effect has ever been observed in supported or unsupported polymer films. In addition, the 47 K reduction in T_g relative to $T_{g,bulk}$ observed in the 25 nm thick PTBS film is the largest T_g reduction observed experimentally in supported polymer films.

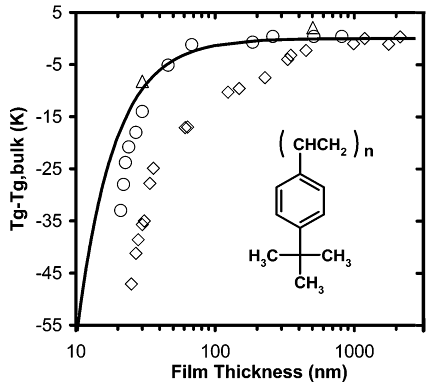

Figure 7. $T_g - T_{g,bulk}$ as a function of film thickness for P4MS (○) films as measured by pyrene dopant fluorescence, PTBS (◇) films as measured by BPD dopant fluorescence, and PS (△) (M_n = 200 000 g/mol) films as measured by BPD dopant fluorescence. The bold curve represents a fit of the PS data in Figure 3 to the empirical relation of Keddie et al.[7] The inset shows the structure of the PTBS repeat unit.

This strongly enhanced thickness dependence of T_g in PTBS relative to PS and even P4MS demonstrates that there is substantial tunability of the T_g-nanoconfinement effect. These results complement those of ref 25 that first revealed a tunability of the T_g-nanoconfinement effect by the addition of low MW plasticizers, albeit in the opposite direction; i.e., the thickness dependence was reduced or eliminated upon diluent addition. Given the invariance demonstrated in the T_g-nanoconfinement effect as a function of PS MW (from 5000 to 3 000 000 g/mol), such dramatic differences in the impact of confinement on PTBS relative to PS may be considered surprising. However, as the addition of the *tert*-butyl group to PS reduces the bulk density substantially (nearly to that of styrene monomer, which has a density of 0.90 g/cm^3) while resulting in a more rigid chain due to steric effects, it may be unreasonable to expect that there should much similarity in the T_g-nanoconfinement in PS and PTBS, except for the fact that the T_g values are expected to decrease with decreasing thickness below some onset thickness.

Up to the present time, these factors of overall density and chain stiffness have not been described in the literature as being associated with T_g-confinement effects. Here we hypothesize that it is chain stiffness rather than polymer density that may be responsible for or at least is associated with the much more dramatic T_g-nanoconfinement effect in PTBS as compared to PS and P4MS. This hypothesis is supported by a the fact that a recent study[76] reported that polycarbonate, which has significantly greater chain stiffness than PS, exhibits a substantial T_g reduction relative to $T_{g,bulk}$ at a thickness of 142 nm, far greater than that observed for PS or P4MS. Obviously, while interesting issues remain to be explored in this field with PS, it may be possible that much greater insight may be gained by undertaking other studies involving small changes in repeat unit structure like those employed in the present study or in determining the effect of film thickness on T_g on polymers that bear little resemblance to PS and that may be accompanied by major changes in chain stiffness, density, etc. Such studies are currently underway in our laboratory.

C. Comparison of the Length Scale of Cooperative Dynamics for PS as a Function of MW and Repeat Unit Structure to the T_g-Nanoconfinement Behavior. In a recent study that discussed the determination of the distribution of T_g values in nanoconfined PS,[24] it was shown that the free-surface effect results in a significantly reduced local T_g (by some tens of degrees) at the free surface and that the local T_g is perturbed from its bulk value in buried layers located several tens of nanometers into the film interior. From these results, it may be rationalized that the T_g-nanoconfinement effect in supported PS films results from two things: (1) a significant perturbation in local segmental dynamics at the free-surface interface and (2) a mechanism by which these free-surface effects may propagate into the film interior. It is clear from ref 24 that there is not a one-to-one relationship between the length scale of a CRR at T_g and the length scale from the free surface over which T_g dynamics are modified and thus not a one-to-one relationship between the length scale of a CRR and the onset thickness at which the T_g-nanoconfinement effect is observed. However, as yet unresolved is the issue of whether there is some even qualitatively definable relationship between the length scale of a CRR at T_g in the unperturbed bulk polymer and the other two length scales. (Furthermore, a recent perspective article[77] has indicated that cooperativity length scales have been insufficiently studied in regard to their potential connection to T_g dynamics in confinement.)

Here we address this issue by determining the size of a single CRR at $T_{g,bulk}$, ξ_{CRR}, using the thermal fluctuation theory and DSC method by Donth.[47−49,78] In this approach

$$V_{CRR} = {\xi_{CRR}}^3 = k_B T_g(\text{mid})^2 \Delta(1/C_v)/(\rho \delta T^2) \qquad (1)$$

where V_{CRR} is the volume of one CRR, ξ_{CRR} is the size (length scale) of one CRR, k_B is the Boltzmann constant, T_g(mid) is the Richardson midpoint T_g, $\Delta(1/C_v)$ is the step change in $1/C_v$ at the dynamic T_g, ρ is the density of bulk polymer, δT is the mean temperature fluctuation of one average CRR, and C_v is the heat capacity at constant volume. It must be noted that actual calculations employing the DSC method involve the approximation[47,48] that $\Delta(1/C_v)$ can be replaced by $\Delta(1/C_p)$, where C_p is the heat capacity at constant pressure, a quantity that may be measured by DSC. In turn, $\Delta(1/C_p)$ is taken as being equivalent to $\Delta C_p/{C_p}^2$. (This approximation has been estimated by Donth to lead, on average, to a slight overestimation of V_{CRR}. This is discussed further in ref 79.) The number of units present in one CRR (N_{CRR}) is given by the following:

$$N_{CRR} = (\rho V_{CRR} N_a)/M_0 \qquad (2)$$

where N_a is Avogadro's number and M_0 is the MW of a single repeat unit. More specific details regarding the determinations of ξ_{CRR} and N_{CRR} may be found in the Supporting Information.

Donth's approach has been described in the literature as being controversial[56] because the associated theoretical analysis has not been verified. While acknowledging this point, we note that the experiments are straightforward and, when a reasonable temperature dependence for the cooperativity length scale is assumed, result in estimates of ξ_{CRR} that are consistent with the very few measurements of ξ_{CRR} obtained by 4D-NMR methods. For example, using eq 1 we have determined a value of ~3.3 nm[80] for ξ_{CRR} for glycerol at T_g, allowing us to draw comparisons to results obtained for glycerol above T_g via 4D-NMR. (See Table 2 for the values of

Table 2. Sample Parameter Values Leading to the Calculation of ξ_{CRR}[86] and N_{CRR}

system	ΔC_p (J/(g K))	C_p (J/(g K))	δT (K)	T_g(mid) (K)	ξ_{CRR}[d] (nm)	N_{CRR}[e]
PS[a]	0.411	1.375	2.84	270	3.0	160
PS[b]	0.277	1.873	1.90	377	3.5	255
P4MS	0.254	1.819	2.03	385	3.3	195
PTBS	0.226	2.119	2.61	405	2.6	65
PS[c]+ 4 wt % DOP	0.270	1.629	2.65	362	3.0	160
glycerol	0.944	1.394	2.23	188	3.3	315

[a] M_n = 800 g/mol. [b] M_n = 3 000 000 g/mol. [c] M_n = 400 000 g/mol. [d] ξ_{CRR} values have been truncated to one digit after the decimal place. [e] N_{CRR} values have been rounded to the nearest 5. Note: Details regarding the standard deviations associated with the parameters above may be found in the Supporting Information associated with this paper.

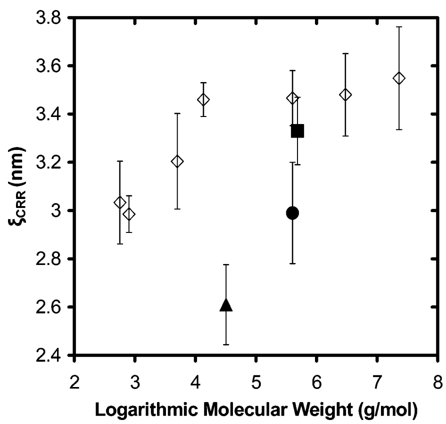

Figure 8. ξ_{CRR} values[86] as a function of logarithmic molecular weight for PS (◇), P4MS (■), PtBS (▲), and PS (M_n = 400 000 g/mol) doped with 4 wt % dioctyl phthalate (●). Error bars indicate the standard deviation about the mean of measured ξ_{CRR} values for that MW of PS or other polymer.

the parameters in eq 1. Also see the Supporting Information for this paper for details regarding how the values of some of the parameters were obtained.) Using 4D-NMR[53,54] and their most recent analysis of the data, Speiss and co-workers[81] report ξ_{CRR} values for glycerol of 1.3 ± 0.5 nm at T_g + 10 K, 1.1 ± 0.5 nm at T_g + 14 K, and 1.0 ± 0.5 nm at T_g + 18 K.

A direct comparison of ξ_{CRR} values obtained by Donth's approach and 4D-NMR cannot be made at the same temperature as the former method yields data at T_g while the latter method has been applied in a certain dynamic range associated with temperatures closer to T_g + 10 K. Employing a dynamic scaling approach and results from dielectric spectroscopy studies by others,[82,83] Erwin and Colby[56] provide data indicating that ξ_{CRR} for glycerol increases by ~80% as temperature is decreased from T_g + 10 K to T_g. Applying this factor to the data by Spiess and co-workers, we estimate a value of ξ_{CRR} of 1.44−3.24 nm for glycerol at T_g. Given that there is a substantial uncertainty associated with our estimate of 3.3 nm using Donth's method (see ref 79 and further discussion below), it is possible to conclude that, when the effects of temperature difference are taken into account, determinations of ξ_{CRR} by 4D-NMR and Donth's approach are consistent with each other.[84]

Based on our DSC measurements and eq 1, Figure 8 shows the effect of PS MW on the value of ξ_{CRR} over a MW range of 568−23 000 000 g/mol, an even broader MW range than employed in section A. This is also a broader MW range than that investigated 20 years ago by Donth[49,85] in the only other study of the MW dependence of ξ_{CRR} for PS at T_g. Figure 8 also includes the first determinations of the ξ_{CRR} values for P4MS, PTBS, and PS containing 4 wt % dioctyl phthalate (DOP) plasticizer. The latter system is identical to one studied in ref 25 that revealed that the T_g-nanoconfinement effect can be essentially eliminated down to film thicknesses of 14 nm by diluent addition to PS. Within our range of experimental error, the size of the CRR for PS is ~3.5 nm,[86] invariant with MW from 23 000 000 g/mol at least down to M_n values of 13 500 g/mol. (See Table 2 for examples of parameter values that are required to determine ξ_{CRR} using eq 1.) Given the sizes of error bars in Figure 8, a case may even be made that within experimental error the size of the CRR is invariant with PS MW down to M_n values of 5000 g/mol. This value of the CRR size in PS at $T_{g,bulk}$ is slightly larger than the value of 3.0 nm recently reported by Donth and co-workers[48] using regular DSC methods similar to those employed in our study. Most of this difference is due to the level of inaccuracy of the assumption that $\Delta(1/C_v) \approx \Delta(1/C_p)$, where C_p is measured by DSC. In ref 48, Donth and co-workers "correct" the $\xi_{CRR}{}^3$ data for this inaccuracy by a common factor of 0.74[79] across all data (both low MW and polymeric glass formers). We have not made a similar adjustment to the data here in order to avoid overgeneralization, especially as we do not know the correction factor for each system employed in our study. However, we note that if we had used Donth's correction factor, it would have resulted in a value of ξ_{CRR} = 3.1−3.2 nm for our PS data, almost in exact agreement with Donth's value of 3.0 nm given in ref 48 (see ref 79).

In addition, the approach for determining the size of the CRR using a regular DSC method involves some "rules of thumb" for determining the δT parameter prescribed by Donth (rather than the more rigorous method by Donth involving determination of δT from the Kohlrausch−Williams−Watts exponent in conjunction with measurements by thermally modulated DSC). With the application of these rules of thumb, Donth has argued[48] that the accuracy of the characteristic size of a CRR is within 85% and 125% of the calculated value. (See Supporting Information associated with this paper for further details.) Thus, according to Donth's expectations for accuracy of the method, we can argue that for nonoligomeric PS the value of ξ_{CRR} is between 3.0 and 4.4 nm. (These values do not include Donth's factor correcting for the average inaccuracy of the assumption that $\Delta(1/C_v) = \Delta(1/C_p)$.) While this range of values for ξ_{CRR} may seem large, it is less than that estimated from 4D-NMR determinations of the size of a CRR for PVAc (3.7 ± 1 nm).[81]

Figure 8 also illustrates that when the PS MW is reduced to oligomeric systems with MWs 568 or 800 g/mol, the experimentally determined ξ_{CRR} value is, outside of our experimental uncertainty as described by our error bars, reduced from that of our higher MW PS samples, taking on a value of ~3.0 nm.[86] The fact that the size of a CRR is, within experimental error, invariant with PS MW until the MW is sufficiently reduced to yield an oligomer (or nearly an oligomer) is reasonably consistent with studies[87−90] on the MW dependence of the fragility index or related behavior for PS. The fragility index m can defined by the value of d $\log(\tau)/\mathrm{d}(T_g/T)$ evaluated in the equilibrium rubbery or liquid state in the limit of $T = T_g$, where τ is the average α-relaxation time or the average relaxation time of the cooperative segmental dynamics associated with T_g.[91] Often the value of m is determined at a fixed value of τ associated with T_g, e.g., 100 s. The fragility index may be regarded as another measure of the nature of the cooperative motion and has been described[87] as being a "...reflection of the effect intermolecular cooperativity has on the (segmental) dynamics." A couple of studies concerning the MW dependence of the fragility index for PS have yielded the following picture: oligomeric PS (e.g., 590[87] and 1100 g/mol[88]) exhibits a major reduction in the fragility index (or related parameters such as Ngai's coupling parameter[88]) relative to high MW PS although some MW dependence to the fragility index is exhibited at MWs as high as 6400 g/mol.[87]

Given the definitions of the size of an average CRR at T_g and the fragility index, for a particular glass-forming system both values are expected to decrease with a decrease in the number of units involved in cooperative segmental mobility at T_g. In the case of PS, oligomers are expected to have a reduced requirement for cooperative segmental mobility at T_g because of the dramatically reduced connectivity between repeat units and increase in free volume that are manifested in large reductions of T_g relative to high MW PS. However, the extent to which the values of ξ_{CRR} and m are reduced with reductions in the cooperativity of a particular system may differ substantially. It has been suggested[92,93] that a value such as m reflects the apparent activation energy associated with cooperative segmental mobility in the rubbery state in the limit of $T = T_g$. This is expected to be related to the number of units involved in cooperative segmental mobility and thereby the volume of the CRR rather than the size of the CRR. Thus, m is expected to exhibit a greater change than ξ_{CRR} with cooperativity requirements at T_g.

The experimentally measured reduction in the value of ξ_{CRR} from ~3.5 to ~3.0 nm[86,94] upon addition of 4 wt % dioctyl phthalate to PS is also consistent with experimental observation of a reduction in fragility with diluent addition.[88] The reduction in the size of the CRR with diluent addition is expected based on the fact that the presence of diluent reduces constraints associated with cooperative segmental motion.

In contrast to the easily explained result for diluent addition, the effect of small changes to the repeat unit structure of PS on the size of the CRR is not as easily rationalized. The value of ξ_{CRR} obtained for P4MS is ~3.4 nm,[86] within experimental error the same as that of PS. It is possible that the difference in repeat unit structure between PS and P4MS results in a small enough perturbation to cooperative segmental mobility that it is not evident in measurements of ξ_{CRR}. In contrast, the value of ξ_{CRR} obtained for PTBS is ~2.6 nm[86] which, outside of experimental error, is even smaller than that observed for oligomeric PS. From inspection of the structures of PS and P4MS, it would be logical to assume that, other things being equal, the presence of the *tert*-butyl group in PTBS would greatly increase the cooperativity requirements relative to PS. However, other things are not equal in these two systems, as the 10% reduction in density of PTBS relative to PS easily attests. Thus, the *tert*-butyl groups in PTBS greatly reduce the packing efficiency of the repeat units relative to PS, and it is surmised that this packing effect may overcome the expectation of increased cooperativity (in the absence of free volume effects) and result in a net major reduction in the size of an average cooperatively rearranging region at T_g.[95] Further study of these issues in related systems is warranted.

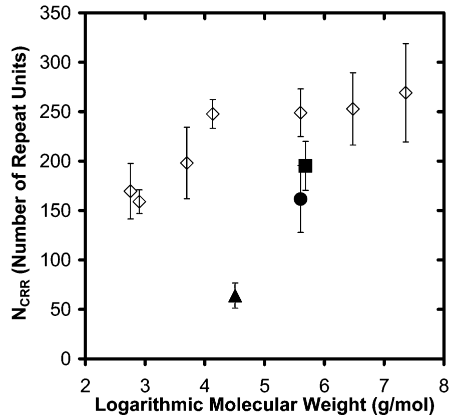

Figure 9. N_{CRR} values[86] as a function of logarithmic molecular weight for PS (◇), P4MS (■), PtBS (▲), and PS (M_n = 400 000 g/mol) doped with 4 wt % dioctyl phthalate (●). Error bars indicate the standard deviation about the mean of measured N_{CRR} values for that MW of PS or other polymer.

To better appreciate the importance of packing efficiency relative to that of polymer MW in dictating the cooperativity required at T_g, Figure 9 plots the number of repeat units associated with an average CRR, N_{CRR}, as a function of polymer MW. The value of N_{CRR} was calculated making the assumption that the volume of a CRR is cubic in nature (which we understand oversimplifies the shape of a CRR) and taking into account the exact density of the polymers involved; thus, the important quantitative information in Figure 9 relates to how the N_{CRR} values depend on a particular parameter instead of the exact values of the N_{CRR}. The oligomeric PS samples have N_{CRR} values that are ~60−70% that of higher MW PS, in reasonable agreement with 20 year old data of Donth,[49] who found a MW dependence of N_{CRR} for PS at T_g similar to that shown in Figure 9. (Donth actually reported MW per CRR rather than N_{CRR}.) Most striking in Figure 9 is the fact that the PTBS sample has an N_{CRR} value that is 20−30% that of high MW PS. Similarly large differences among different polymers have been observed by Donth and co-workers,[48] who reported that poly(*n*-alkyl methacrylates) have dramatically reduced values of N_{CRR} relative to other polymers including PS.

We also note that two recent studies have employed the DSC method of Donth to investigate the values of ξ_{CRR} and N_{CRR} or V_{CRR} for PS[50] and poly(methyl methacrylate) (PMMA)[51] as a function of confinement in clay nanocomposites. Both studies reported an increase of T_g in the nanocomposite relative to neat polymer. However, the PS study reported a 75% increase in V_{CRR}, equivalent to about a 20% increase in ξ_{CRR}, upon confinement in the nanocomposite while the PMMA study reported about a 20% decrease in ξ_{CRR} upon confinement in the nanocomposite. The different trends in these two studies suggest that at present there is not a qualitative correlation between ξ_{CRR} and modification of T_g in nanocomposites.

With the results provided in Figures 8 and 9, it is possible to address the issue of whether a simple qualitative relationship exists between the size of a CRR at $T_{g,bulk}$ and the T_g-nanoconfinement effect. At one level, the invariance of ξ_{CRR} and N_{CRR} with PS MW (except for oligomeric PS) is in accord with absence of a MW effect to the T_g-nanoconfinement effect in supported PS films. However, while large reductions in the values of ξ_{CRR} and N_{CRR} are observed in PTBS and PS with 4 wt % DOP relative to the values observed in neat PS, PTBS exhibits a major enhancement of the T_g-nanoconfinement effect relative to PS while the PS with 4 wt % DOP exhibits an elimination of the effect down to a film thickness of 14 nm.[25] Thus, the present results do not allow for a description of a "rule of thumb" regarding how a change in the size of the CRR in bulk polymer relates to the tunability of the T_g-nanoconfinement effect. However, we believe that the impact of modifications to the repeat unit structure on the nature of the polymer dynamics at the air–polymer interface as well as how such modifications impact the manner in which the perturbation to dynamics at the free surface propagate into the film interior may hold the answer. Studies of such issues as well as novel investigations to determine the general impact of interfaces on the cooperative segmental mobility (e.g., the full α-relaxation time distribution) in conjunction with repeat unit structural modifications may be key in gaining a better understanding of the T_g-nanoconfinement effect.

Conclusions

The effect of nanoconfinement on the T_g of PS films is investigated over the broadest MW range ever reported in a single study (5000–3 000 000 g/mol). In contrast to two recent reports,[20,21,69] here it is observed that PS MW has no significant impact on the film thickness dependence of $T_g - T_{g,bulk}$. This result is consistent with the substantial evidence in the literature, indicating that T_g-nanoconfinement effects originate from interfaces and surfaces which impact the cooperative segmental mobility associated with T_g and are not due to other factors which may depend on MW such as degree of chain end segregation, entanglement density, etc. In contrast, small modifications to the repeat unit structure of PS are observed to have a dramatic impact on the T_g-nanoconfinement effect. A stronger film thickness dependence of T_g is observed for P4MS compared to PS, while PTBS exhibits a stronger dependence than both PS and P4MS. The T_g reduction for a 25 nm thick PTBS film is 47 K relative to $T_{g,bulk}$, which is the largest reduction from $T_{g,bulk}$ ever observed for supported polymer films. Furthermore, the onset thickness for the T_g-nanoconfinement effect is 300–400 nm in PTBS, the largest thickness for which such a confinement effect has been reported. These results, along with those reported in ref 25 related to the reduction or elimination of T_g-nanoconfinement effects via diluent addition, indicate that small changes in the polymer system, with the exception of MW, can yield major changes in the impact of confinement on T_g behavior.

The characteristic dynamics of the cooperative motion associated with T_g is examined via the size of a CRR at T_g, ξ_{CRR}. The value of ξ_{CRR} is approximately independent of PS MW over the same range of MWs for which the T_g-nanoconfinement effect is MW invariant. However, other system variations such as modification of repeat unit structure yield changes in ξ_{CRR} values of bulk polymer systems that do not correlate in an obvious manner with the strength of the T_g-nanoconfinement effect. For example, both the PS + 4 wt % DOP system and PTBS exhibit reduced values of ξ_{CRR} relative to PS; however, PS + 4 wt % DOP exhibits no T_g-nanoconfinement effect down to a film thickness of 14 nm,[25] while PTBS exhibits the onset of the effect at a thickness of 300–400 nm in supported films. Future studies related to how free surfaces and interfaces impact cooperative segmental dynamics as a function of polymer repeat unit structure and diluent addition are warranted.

Acknowledgment. This work was supported by the NSF-MRSEC program (Grant DMR-0076097), Northwestern University, a Henderson Dissertation-Year Fellowship (to C.J.E.), and a Murphy Fellowship (to M.K.M.). We also acknowledge the use of equipment in shared user facilities managed by the Materials Research Center at Northwestern University.

Supporting Information Available: Details of the calculations of ξ_{CRR} and N_{CRR}. This material is available free of charge via the Internet at http://pubs.acs.org.

References and Notes

(1) Jackson, C. L.; McKenna, G. B. *J. Non-Cryst. Solids* **1991**, *131–133*, 221–224.
(2) Arndt, M.; Stannarius, R.; Groothues, H.; Hempel, E.; Kremer, F. *Phys. Rev. Lett.* **1997**, *79*, 2077–2080.
(3) Barut, G.; Pissis, P.; Pelster, R.; Nimtz, G. *Phys. Rev. Lett.* **1998**, *80*, 3543–3546.
(4) Melnichenko, Y. B.; Schuller, J.; Richert, R.; Ewen, B.; Loong, C. K. *J. Chem. Phys.* **1995**, *103*, 2016–2024.
(5) Schonhals, A.; Goering, H.; Schick, C. *J. Non-Cryst. Solids* **2002**, *305*, 140–149.
(6) Wang, L. M.; He, F.; Richert, R. *Phys. Rev. Lett.* **2004**, *92*, 095701-1–095701-4.
(7) Keddie, J. L.; Jones, R. A. L.; Cory, R. A. *Europhys. Lett.* **1994**, *27*, 59–64.
(8) Keddie, J. L.; Jones, R. A. L.; Cory, R. A. *Faraday Discuss.* **1994**, *98*, 219–230.
(9) van Zanten, J. H.; Wallace, W. E.; Wu, W. L. *Phys. Rev. E* **1996**, *53*, R2053–R2056.
(10) Kawana, S.; Jones, R. A. L. *Phys. Rev. E* **2001**, *63*, 021501–1–021501–6.
(11) DeMaggio, G. B.; Frieze, W. E.; Gidley, D. W.; Zhu, M.; Hristov, H. A.; Yee, A. F. *Phys. Rev. Lett.* **1997**, *78*, 1524–1527.
(12) Fukao, K.; Miyamoto, Y. *Phys. Rev. E* **2000**, *61*, 1743–1754.
(13) Forrest, J. A.; Dalnoki-Veress, K.; Dutcher, J. R. *Phys. Rev. E* **1997**, *56*, 5705–5716.
(14) Forrest, J. A.; Dalnoki-Veress, K. *Adv. Colloid Interface Sci.* **2001**, *94*, 167–196.
(15) Grohens, Y.; Hamon, L.; Reiter, G.; Soldera, A.; Holl, Y. *Eur. Phys. J. E* **2002**, *8*, 217–224.
(16) Pham, J. Q.; Green, P. F. *J. Chem. Phys.* **2002**, *116*, 5801–5806.
(17) Sharp, J. S.; Forrest, J. A. *Phys. Rev. Lett.* **2003**, *91*, 235701-1–235701-4.
(18) Tsui, O. K. C.; Zhang, H. F. *Macromolecules* **2001**, *34*, 9139–9142.
(19) Kim, J. H.; Jang, J.; Zin, W. C. *Langmuir* **2001**, *17*, 2703–2710.
(20) Singh, L.; Ludovice, P. J.; Henderson, C. L. *Thin Solid Films* **2004**, *449*, 231–241.
(21) Miyazaki, T.; Nishida, K.; Kanaya, T. *Phys. Rev. E* **2004**, *69*, 061803-1–061803-6.
(22) Ellison, C. J.; Kim, S. D.; Hall, D. B.; Torkelson, J. M. *Eur. Phys. J. E* **2002**, *8*, 155–166.
(23) Ellison, C. J.; Torkelson, J. M. *J. Polym. Sci., Part B: Polym. Phys.* **2002**, *40*, 2745–2758.
(24) Ellison, C. J.; Torkelson, J. M. *Nat. Mater.* **2003**, *2*, 695–700.

(25) Ellison, C. J.; Ruszkowski, R. L.; Fredin, N. J.; Torkelson, J. M. *Phys. Rev. Lett.* **2004**, *92*, 095702-1−095702-4.
(26) Forrest, J. A.; Dalnoki-Veress, K.; Dutcher, J. R. *Phys. Rev. E* **1998**, *58*, 6109−6114.
(27) Forrest, J. A.; Mattsson, J. *Phys. Rev. E* **2000**, *61*, R53−R56.
(28) Forrest, J. A.; Dalnoki-Veress, K.; Stevens, J. R.; Dutcher, J. R. *Phys. Rev. Lett.* **1996**, *77*, 2002−2005.
(29) Dalnoki-Veress, K.; Forrest, J. A.; Murray, C.; Gigault, C.; Dutcher, J. R. *Phys. Rev. E* **2001**, *63*, 031801-1−031801-10.
(30) Fukao, K.; Miyamoto, Y. *Europhys. Lett.* **1999**, *46*, 649−654.
(31) Fukao, K.; Uno, S.; Miyamoto, Y.; Hoshino, A.; Miyaji, H. *J. Non-Cryst. Solids* **2002**, *307*, 517−523.
(32) D'Amour, J. N.; Okoroanyanwu, U.; Frank, C. W. *Microelect. Eng.* **2004**, *73*−*74*, 209−217.
(33) Park C. H.; Kim, J. H.; Ree, M.; Sohn, B. H.; Jung, J. C.; Zin, W. *Polymer* **2004**, *45*, 4507−4513.
(34) Pham, J. Q.; Green, P. F. *Macromolecules* **2003**, *36*, 1665−1669.
(35) Fryer, D. S.; Peters, R. D.; Kim, E. J.; Tomaszewski, J. E.; de Pablo, J. J.; Nealey, P. F.; White, C. C.; Wu, W. L. *Macromolecules* **2001**, *34*, 5627−5634.
(36) Tsui, O. K. C.; Russell, T. P.; Hawker, C. J. *Macromolecules* **2001**, *34*, 5535−5539.
(37) Hall, D. B.; Hooker, J. C.; Torkelson, J. M. *Macromolecules* **1997**, *30*, 667−669.
(38) McKenna, G. B. *J. Phys. IV* **2000**, *10*, 53−57.
(39) Bernazzani, P.; Simon, S. L.; Plazek, D. J.; Ngai, K. L. *Eur. Phys. J. E* **2002**, *8*, 201−207.
(40) Adam, G.; Gibbs, J. H. *J. Chem. Phys.* **1965**, *43*, 139−146.
(41) Brown, H. R.; Russell, T. P. *Macromolecules* **1996**, *29*, 798−800.
(42) Mayes, A. M. *Macromolecules* **1994**, *27*, 3114−3115 and references therein.
(43) It should be noted that it is unclear whether the appropriate T_g scaling is in terms of a departure from bulk T_g as $T_g(h) - T_{g,\ bulk}$ or in terms of a reduced T_g as $T_g(h)/T_{g,\ bulk}$.
(44) Kanaya, T.; Miyazaki, T.; Watanabe, H.; Nishida, K.; Yamano, H.; Tasaki, S.; Bucknall, D. B. *Polymer* **2003**, *44*, 3769−3773.
(45) Orts, W. J.; van Zanten, J. H.; Wu, W. L.; Satija, S. K. *Phys. Rev. Lett.* **1993**, *71*, 867−870.
(46) Soles, C. L.; Douglas, J. F.; Jones, R. L.; Wu, W. L. *Macromolecules* **2004**, *37*, 2901−2908.
(47) Donth, E. *J. Polym. Sci., Part B: Polym. Phys.* **1996**, *34*, 2881−2892.
(48) Hempel, E.; Hempel, G.; Hensel, A.; Schick, C.; Donth, E. *J. Phys. Chem. B* **2000**, *104*, 2460−2466.
(49) Donth, E. *Acta Polym.* **1984**, *35*, 120−123.
(50) Vyazovkin, S.; Dranca, I. *J. Phys. Chem. B* **2004**, *108*, 11981−11987.
(51) Tran, T. A.; Said, S.; Grohens, Y. *Polym. Mater. Sci. Eng.* **2004**, *91*, 677−678.
(52) Robertson, C. G.; Wang, X. R. *Macromolecules* **2004**, *37*, 4266−4270.
(53) Tracht, U.; Wilhelm, M.; Heuer, A.; Feng, H.; Schmidt-Rohr, K.; Spiess, H. W. *Phys. Rev. Lett.* **1998**, *81*, 2727−2730.
(54) Reinsberg, S. A.; Qiu, X. H.; Wilhelm, M. Spiess, H. W.; Ediger, M. D. *J. Chem. Phys.* **2001**, *114*, 7299−7302.
(55) Hong, P. D.; Chuang, W. T.; Yeh, W. J.; Lin, J. L. *Polymer* **2002**, *43*, 6879−6886.
(56) Erwin, B. M.; Colby, R. H. *J. Non-Cryst. Solids* **2002**, *307*−*310*, 225−231.
(57) Jain, T. S.; de Pablo, J. J. *Phys. Rev. Lett.* **2004**, *92*, 155505-1−155505-4.
(58) Herminghaus, S.; Seeman, R.; Landfester, K. *Phys. Rev. Lett.* **2004**, *93*, 017801-1−017801-4.
(59) Merabia, S.; Sotta, P.; Long, D. *Eur. Phys. J. E* **2004**, *15*, 189−210.
(60) Schwab, A. D.; Agra, D. M. G.; Kim, J. H.; Kumar, S.; Dhinojwala, A. *Macromolecules* **2000**, *33*, 4903−4909.
(61) Jean, Y. C.; Zhang, R.; Cao, H.; Yuan, J. P.; Huang, C. M. *Phys. Rev. B* **1997**, *56*, R8459−R8462.
(62) Torres, J. A.; Nealey, P. F.; de Pablo, J. J. *Phys. Rev. Lett.* **2000**, *85*, 3221−3224.
(63) Pochan, D. J.; Lin, E. K.; Satija, S. K.; Wu, W. L. *Macromolecules* **2001**, *34*, 3041−3045.
(64) Kajiyama, T.; Tanaka, K.; Takahara, A. *Macromolecules* **1997**, *30*, 280−285.
(65) Sperling, L. H. *Introduction to Physical Polymer Science,* 2nd ed.; Wiley-Interscience: New York, 1992.
(66) Majeste, J. C.; Montfort, J. P.; Allal, A.; Marin, G. *Rheol. Acta* **1998**, *37*, 486-499.
(67) Flory, P. J. *Statistical Mechanics of Chain Molecules*; Hanser Publishers: Munchen, 1989.
(68) The overall chain conformation is likely substantially altered in nanoconfined films, adopting, on average, an ellipsoidal conformation with a large aspect ratio as opposed to the random coil expected in bulk.
(69) It should be noted that both refs 20 and 21 have measured T_g upon heating from the glassy state after prior annealing at 408 K for 20−48 h[20] or 423 K for 48 h.[21]
(70) Hall, D. B.; Underhill, P.; Torkelson, J. M. *Polym. Eng. Sci.* **1998**, *38*, 2039−2045.
(71) Vigil, M. R.; Bravo, J.; Atvars, T. D. Z.; Baselga, J. *Macromolecules* **1997**, *30*, 4871−4876.
(72) Brown, G. O.; Atvars, T. D. Z.; Guardala, N. A.; Price, J. L.; Weiss, R. G. *J. Polym. Sci., Part B: Polym. Phys.* **2004**, *42*, 2957−2970.
(73) Kawana, S.; Jones, R. A. L. *Eur. Phys. J. E* **2003**, *10*, 223−230.
(74) Priestley, R. D.; Broadbelt, L. J.; Torkelson, J. M. *Macromolecules* **2005**, *38*, 654−657.
(75) Deppe, D. D.; Miller, R. D.; Torkelson, J. M. *J. Polym. Sci., Part B: Polym. Phys.* **1996**, *34*, 2987−2997.
(76) Soles, C. L.; Douglas, J. F.; Wu, W. L.; Peng, H.; Gidley, D. W. *Macromolecules* **2004**, *37*, 2890−2900.
(77) McKenna, G. B. *Eur. Phys. J. E* **2003**, *12*, 191−194.
(78) It should be noted that Donth's method has been described in the literature (see ref 56) as being controversial as it theoretical basis has not been verified.
(79) The error in this estimation may be summarized by a parameter S where $S = \Delta(1/C_v)/\Delta(1/C_p)$. Donth estimated $S = 0.74 \pm 0.22$ for 14 different polymers and four different small molecule glass formers with the S value extrema at 1.07 and 0.26. Donth has used this average S parameter to correct all values of V_{CRR} and $\xi_{CRR}{}^3$ by S. However, we have not made this correction to our V_{CRR} and $\xi_{CRR}{}^3$ data in order to avoid overgeneralization regarding how $\Delta(1/C_p)$ relates to $\Delta(1/C_v)$ for all our samples. This factor of S nearly exactly accounts for the difference between our ξ_{CRR} value of ~3.5 nm for PS and that measured by Donth of ~3.0 nm.
(80) Given the assumptions employed in Donth's method (see ref 79), the associated error significantly exceeds ±0.1 nm.
(81) Reinsberg, S. A.; Heuer, A.; Doliwa, B.; Zimmermann, H.; Spiess, H. W. *J. Non-Cryst. Solids* **2002**, *307*−*310*, 208−214.
(82) Stickel, F. Doctoral Dissertation, Mainz University, Germany, 1995.
(83) Menon, N.; O'Brien, K. P.; Dixon, P. K.; Wu, L.; Nagel, S. R.; Williams, B. D.; Carini, J. P. *J. Non-Cryst. Solids* **1992**, *141,* 61−65.
(84) We acknowledge discussion in ref 54 that indicates there is inconsistency between ξ_{CRR} values for glycerol obtained by Donth (which are consistent with our data) and those obtained using 4D NMR. However, that discussion invokes the use of a temperature dependence for the size scale or number of units in a cooperatively rearranging region that is different from that mentioned in our paper.
(85) While Donth reported in 1984 (see ref 49) on the MW dependence of the size of a CRR in PS at T_g, we had a couple of reasons for believing that it was important to perform our own investigation of this issue. First, we needed to establish credibility for our experiments, which also included the effects of diluent addition to PS and modification of repeat unit structure. Second, ref 49 has been virtually forgotten in the research literature, even by Donth himself, who has not cited this reference in his later studies. This led to some concern on our part regarding the reference; those concerns were allayed by our measurements. (It should be noted that the results in ref 49 are from analysis of measurements published in: Krause, S.; Iskander, M.; Iqbal, M. *Macromolecules* **1982**, *15*, 105−111).
(86) The values of ξ_{CRR} obtained from our experimental studies are calculated without employing Donth's correction factor, S (see ref 79).
(87) Roland, C. M.; Casalini, R. *J. Chem. Phys.* **2003**, *119*, 1838−1842.
(88) Rizos, A. K.; Ngai, K. L. *Macromolecules* **1998**, *31*, 6217−6225.
(89) Santangelo, P. G.; Roland, C. M. *Macromolecules* **1998**, *31*, 4581−4585.
(90) Robertson, C. G.; Santangelo, P. G.; Roland, C. M. *J. Non-Cryst. Solids* **2000**, *275*, 153−159.

(91) Angell, C. A. *J. Non-Cryst. Solids* **1991**, *131*−*133*, 13−31.
(92) Solunov, C. A. *Eur. Polym. J.* **1999**, *35*, 1543−1556.
(93) Hodge, I. M. *J. Non-Cryst. Solids* **1996**, *202*, 164−172.
(94) In calculating the value of N_{CRR} for the PS + 4 wt % DOP sample, we made the assumption that the density of the system was unaffected by the small amount of DOP diluent. Furthermore, the calculation of N_{CRR} assumed that all units were PS repeat units.
(95) It is highly unlikely that the reductions in N_{CRR} and ξ_{CRR} for PTBS relative to PS have their origins in the values of the S parameter (see ref 79) for PTBS and PS. In order for the values of N_{CRR} and ξ_{CRR} to be approximately the same in the two polymers, the value of the S parameter for PTBS would need to be about 4 times that of PS.

MA047846Y